

# Kent Academic Repository

## Full text document (pdf)

### Citation for published version

Wang, Frank Z. (2017) Fractional memristor. *Applied Physics Letters*, 111 (24). pp. 243502-1. ISSN 0003-6951.

### DOI

<https://doi.org/10.1063/1.5000919>

### Link to record in KAR

<http://kar.kent.ac.uk/65488/>

### Document Version

Publisher pdf

#### Copyright & reuse

Content in the Kent Academic Repository is made available for research purposes. Unless otherwise stated all content is protected by copyright and in the absence of an open licence (eg Creative Commons), permissions for further reuse of content should be sought from the publisher, author or other copyright holder.

#### Versions of research

The version in the Kent Academic Repository may differ from the final published version.

Users are advised to check <http://kar.kent.ac.uk> for the status of the paper. **Users should always cite the published version of record.**

#### Enquiries

For any further enquiries regarding the licence status of this document, please contact:

[researchsupport@kent.ac.uk](mailto:researchsupport@kent.ac.uk)

If you believe this document infringes copyright then please contact the KAR admin team with the take-down information provided at <http://kar.kent.ac.uk/contact.html>

## Fractional memristor

Frank Z. Wang, Luping Shi, Huaqiang Wu, Na Helian, and Leon O. Chua

Citation: *Appl. Phys. Lett.* **111**, 243502 (2017);

View online: <https://doi.org/10.1063/1.5000919>

View Table of Contents: <http://aip.scitation.org/toc/apl/111/24>

Published by the [American Institute of Physics](#)

---

### Articles you may be interested in

[Direct optical observation of spin accumulation at nonmagnetic metal/oxide interface](#)  
*Applied Physics Letters* **111**, 092402 (2017); 10.1063/1.4990113

[Enhanced switching stability in Ta<sub>2</sub>O<sub>5</sub> resistive RAM by fluorine doping](#)  
*Applied Physics Letters* **111**, 092904 (2017); 10.1063/1.4991879

[Magnetic-field-angle dependence of coercivity in CoFeB/MgO magnetic tunnel junctions with perpendicular easy axis](#)  
*Applied Physics Letters* **111**, 132407 (2017); 10.1063/1.5004968

[Photonic-band-gap gyrotron amplifier with picosecond pulses](#)  
*Applied Physics Letters* **111**, 233504 (2017); 10.1063/1.5006348

[Broadband acoustic logic gates in a circular waveguide with multiple ports](#)  
*Applied Physics Letters* **111**, 243501 (2017); 10.1063/1.5004645

[High detectivity visible-blind SiF<sub>4</sub> grown epitaxial graphene/SiC Schottky contact bipolar phototransistor](#)  
*Applied Physics Letters* **111**, 243504 (2017); 10.1063/1.5009003

---

**Scilight**

Sharp, quick summaries **illuminating**  
the latest physics research

Sign up for **FREE!**



## Fractional memristor

Frank Z. Wang,<sup>1,2</sup> Luping Shi,<sup>2</sup> Huaqiang Wu,<sup>2</sup> Na Helian,<sup>3</sup> and Leon O. Chua<sup>4</sup>

<sup>1</sup>School of Computing, University of Kent, Cornwallis South, Canterbury CT2 7NF, United Kingdom

<sup>2</sup>Brain-like Computing Center/Institute of Micro-electronics, Tsinghua University, Beijing 100084, China

<sup>3</sup>School of Computer, University of Hertfordshire, Hatfield AL10 9AB, United Kingdom

<sup>4</sup>Department of Electrical Engineering and Computer Science, University of California, Berkeley, California 94720-1770, USA

(Received 20 August 2017; accepted 10 November 2017; published online 11 December 2017)

Based on the differential conformal transformation in the fractional order, we defined the fractional memristor in contrast to the traditional (integer-order) memristor. As an example, a typical spin-transfer torque (STT) memristor (with the asymmetric resistance hysteresis) was proved to be a 0.8 fractional memristor. In conclusion, many memristors should not be treated as ideal ones due to the fractional interaction between flux and charge. Indeed, unless a non-ideal memristor is properly modelled as a fractional memristor, no deep physical understanding would be possible to develop a reliable commercial product. *Published by AIP Publishing.* <https://doi.org/10.1063/1.5000919>

An (ideal) memristor<sup>1</sup> can be approximated by a piecewise-linear curve (Fig. 1)

$$\varphi = R_P q + \frac{1}{2}(R_{AP} - R_P)[|q + Q_0| - |q - Q_0|], \quad (1)$$

where  $R_{AP}$  denotes the slope of the lower segment,  $R_P$  denotes the slope of the upper segments, and  $q = Q_0$  denotes the charge breakpoint.

The corresponding memristance function  $R(q)$  is derived by differentiating Eq. (1) with respect to  $q$ . The dynamics equations for the above model in the integer-order (it means the order of the differential or the integral is an integer) are as follows:

$$v(t) = R(q)i(t), \quad (2)$$

$$R(q) = R_P + \frac{1}{2}(R_{AP} - R_P)[\text{sgn}(q + Q_0) - \text{sgn}(q - Q_0)], \quad (3)$$

$$\frac{dq(t)}{dt} = i(t) \quad \text{or} \quad q(t) = \int_0^t i(\tau)d\tau, \quad q(0) = 0, \quad (4)$$

where  $\text{sgn}$  is defined by  $\text{sgn}(x) = 1$  if  $x > 0$  and  $\text{sgn}(x) = -1$  if  $x < 0$ .

The memristance depends on the complete past history of the memristor current, i.e., the time integral of the current. Equation (4) represents the memory of  $i(t)$ 's history and is the particular case of the following memory functional when the kernel is the Heaviside function

$$x(t) = k \int_0^t K(t - \tau)i(\tau)d\tau. \quad (5)$$

When  $K(t)$  is the Dirac function,  $x(t) = k i(t)$ , which corresponds to the traditional resistor without any memory effect.

The fractional derivative as a derivative of any arbitrary order was first conceived by Leibniz in 1695.<sup>2</sup> In this work, we will use the differential conformal transformation based on Caputo's derivatives, whose initial conditions are in the same form as for the integer-order differential equations and whose physical meaning is clear.<sup>3-5</sup> Caputo's definition is illustrated as follows:

$${}_0^C D_t^\alpha x(t) = \frac{1}{\Gamma(m - \alpha)} \int_0^t \frac{x^{(m)}(\tau)}{(t - \tau)^{1 + \alpha - m}} d\tau, \quad (6)$$

in which  $m$  is an integer satisfying  $m - 1 < \alpha < m$ . Note that Caputo's definition consists of the memory term similar to Eq. (4).

The Laplace transforms of the Dirac function and the Heaviside function are  $1/s^0$  and  $1/s^1$ , respectively. It is reasonable to describe the non-ideal memristor as  $1/s^\alpha$ , where  $0 < \alpha < 1$ . The inverse Laplace transform of the corresponding kernel  $K(t)$  is

$$K(t) = \frac{t^{\alpha-1}}{\Gamma(\alpha)}. \quad (7)$$

Then,

$$\begin{aligned} x(t) &= k \int_0^t K(t - \tau)i(\tau)d\tau = k \int_0^t \frac{(t - \tau)^{\alpha-1}}{\Gamma(\alpha)} i(\tau)d\tau \\ &= \frac{k}{\Gamma(\alpha)} \int_0^t \frac{1}{(t - \tau)^{1-\alpha}} i(\tau)d\tau = k {}_0 D_t^{-\alpha} i(t). \end{aligned} \quad (8)$$

Therefore, the fractional-order dynamics equations for the (non-ideal) memristor are as follows:

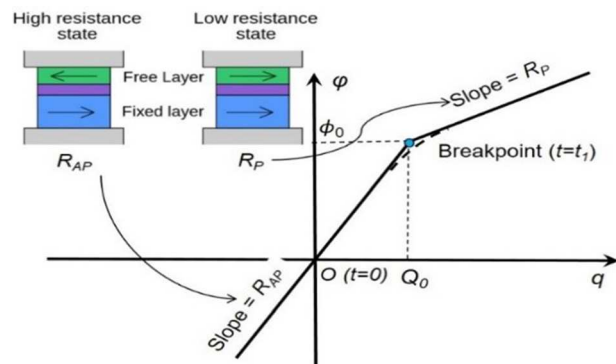


FIG. 1. A piece-wise nonlinear model of a memristor that links directly flux and charge (the coupling between flux and charge could be of a fractional-order). Such a 2-segment memristor is exemplified as a spin-transfer torque (STT) junction (inset) that has the two stable, distinct memristances with abrupt jumps.

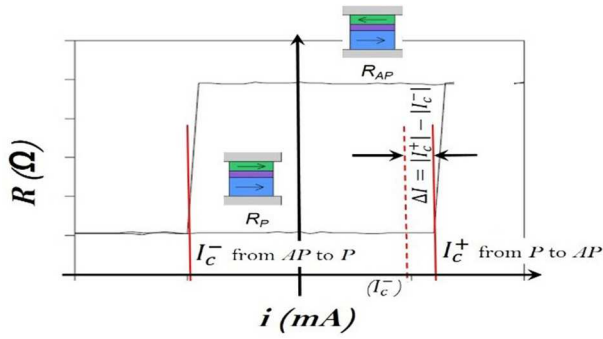


FIG. 2. Many STT junctions display the two stable, distinct memristances with abrupt jumps. Note that a typical  $R$ - $i$  curve based on Refs. 8–11 is shifted by  $\Delta I = |I_c^+| - |I_c^-|$  along the  $i$  axis.  $I_c^+$  represents the critical current corresponding to the switching from  $P$  (Parallel) to  $AP$  (Anti-Parallel), whereas  $I_c^-$  represents the critical current corresponding to the switching from  $AP$  to  $P$ .

$$v(t) = R_\alpha(q)i(t), \tag{9}$$

$$R_\alpha(q) = R_P + \frac{1}{2}(R_{AP} - R_P)[\text{sgn}(q + Q_0) - \text{sgn}(q - Q_0)], \tag{10}$$

$$q(t) = D_t^{-\alpha}i(t), \tag{11}$$

where  $D_t^{-\alpha}i(t)$  represents the memristor's memory effect and  $R_\alpha(q)$  represents the memristor's fractional-order memristance. The above equations reflect a fractional-order coupling between flux and charge.

The above 2-segment memristor could be a spin-transfer torque (STT) junction,<sup>6,7</sup> in which the memristive mechanism is quite universal. Many STT implementations display the two stable, distinct memristances with abrupt jumps.<sup>8,9</sup> Observing Fig. 2 carefully, one can find that the rectangular resistance hysteresis loop  $R$ - $i$  is shifted along the  $i$  axis, resulting in the asymmetric critical switching currents  $|I_c^+| \neq |I_c^-|$ . The observed  $I_c^+$  from  $P$  (Parallel) to  $AP$  (Anti-Parallel) is

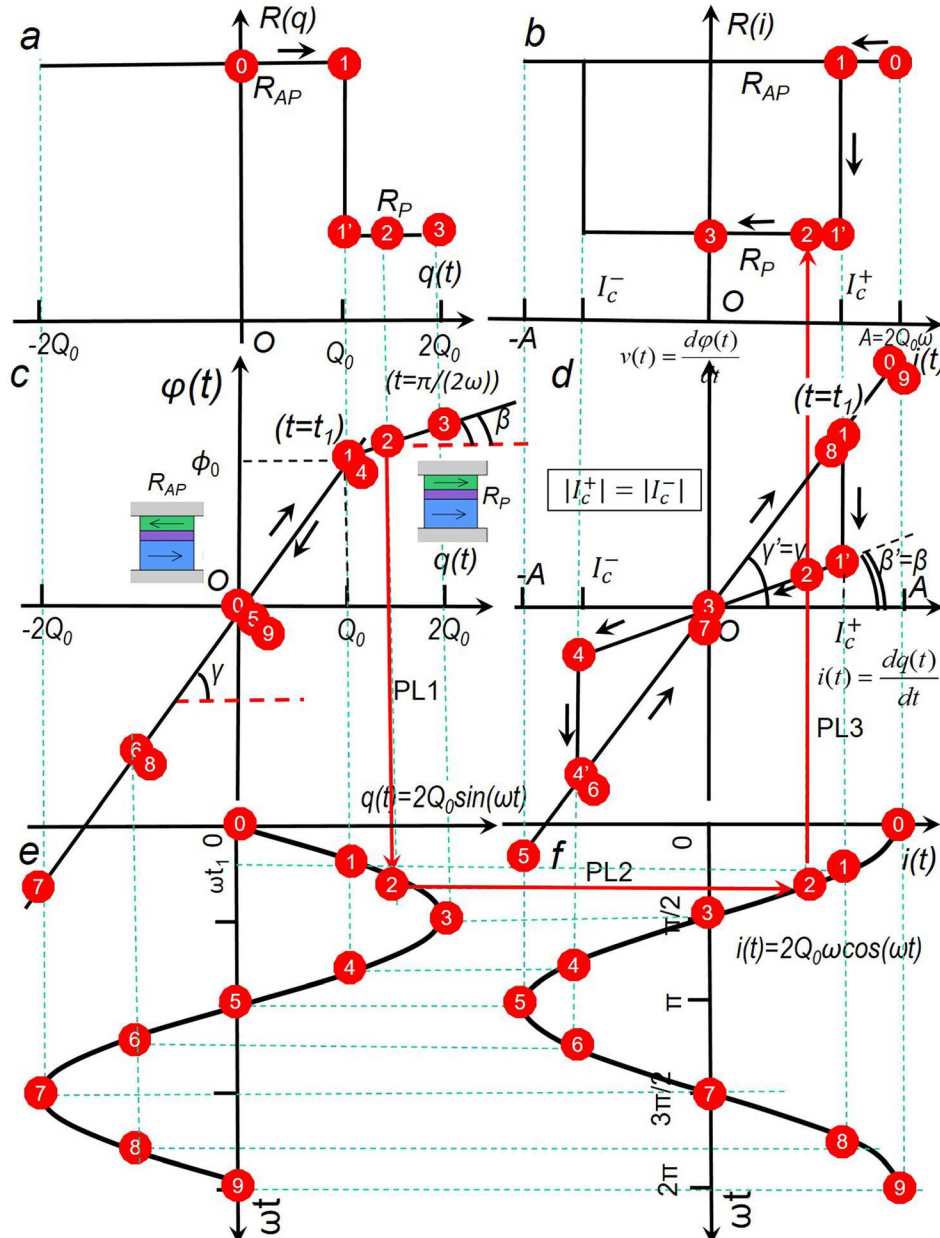


FIG. 3. STT memristor's piecewise-linear model (when the fractional-order  $\alpha=1$ ). The differential conformal transformation projects a given  $\phi$ - $q$  curve for a STT memristor in the  $\phi$ - $q$  plane in (c) onto the  $v$ - $i$  plane in (d),  $R$ - $i$  plane in (b), and  $R$ - $q$  plane in (a). The numbers in red label successive time points. Note that when the fractional-order  $\alpha=1$ , the  $R$ - $i$  curve is symmetric ( $|I_c^+| = |I_c^-|$ ), which is different from the measured one ( $|I_c^+| \neq |I_c^-|$ ) in the STT junction as shown in Fig. 2. Such a difference implies that a real-world STT junction may not be described as an ideal memristor.

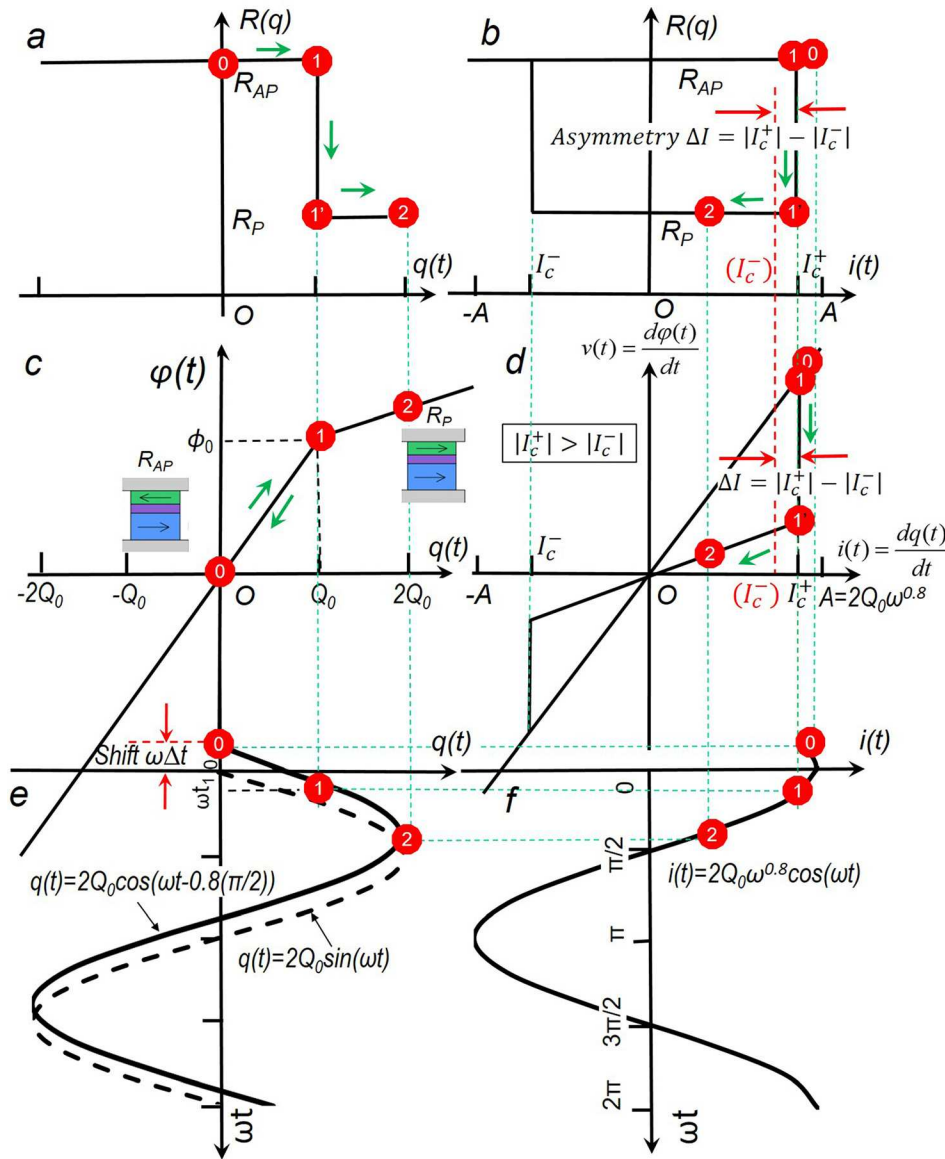


FIG. 4. When the fractional-order  $\alpha = 0.8$ , the shift  $\Delta t$  of  $q(t)$  along the  $t$  axis in (e) causes the asymmetric shifts ( $|I_c^+| \neq |I_c^-|$ ) of the two switching points of the  $v$ - $i$  curves in (d) and  $R$ - $i$  curves in (b) although the breakpoint  $Q_0$  of the  $\varphi$ - $q$  is fixed. The similarity between such an asymmetric rectangular  $R$ - $i$  curve in this figure and the measured one in Fig. 2 reveals that a STT junction is not an ideal memristor, in which  $\alpha = 1$ . Note that the  $v$ - $i$  loci in the fractional-order memristor are also a pinched hysteresis loop through the origin, which is the fingerprint of a memristor.<sup>14</sup>

usually higher than  $I_c^-$  from AP to P, which has been clarified due to the intrinsic difference in the spin transfer torque efficiency for the negative and positive current directions in GMR pillars.<sup>10</sup> Reference 11 also suggests that it is attributed to the different spin accumulation for the two current flow directions and the stray field caused by the fixed layer. In this work, we will use the defined fractional memristor to model the STT junctions as an example.

The differential conformal transformation<sup>12</sup> is vividly illustrated in Fig. 3: a given  $\varphi$ - $q$  curve for a STT memristor in the  $\varphi$ - $q$  plane in (c) is projected onto the  $v$ - $i$  plane in (d) and  $R$ - $i$  plane in (b). This transformation says that the slope ( $\gamma$ ) of the line tangent to the  $\varphi = \hat{\varphi}(q)$  curve at an operating point ( $t = t_0$ ) in the  $\varphi$ - $q$  plane is equal to the slope ( $\gamma'$ ) of a straight line connecting the corresponding point ( $t = t_0$ ) to the origin in the  $v = \hat{v}(i)$  loci (on the same scale as the  $\varphi$ - $q$  plane).

The graphic method for the above transformation is as follows: Draw the voltage-current loci  $v = \hat{v}(i)$  corresponding to the above given  $\varphi = \hat{\varphi}(q)$  curve: (1) Getting  $\gamma$  at an operating point ( $t = t_0$ ) in the  $\varphi = \hat{\varphi}(q)$  curve, we would draw a straight line through the origin in the  $v$ - $i$  plane whose

slope is  $\gamma' = \gamma$ ; and (2) Projecting the point ( $t = t_0$ ) from the  $\varphi$ - $q$  plane onto the  $v$ - $i$  plane by following Projection Lines PL1, PL2 and PL3, we would eventually end up with the same time point ( $t = t_0$ ) in the  $v$ - $i$  plane and the  $R$ - $i$  plane by meeting Projection Line PL3 with the drawn line in the first step.

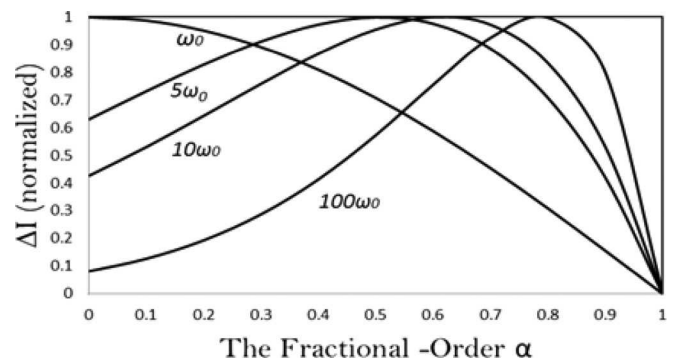


FIG. 5. The asymmetry  $\Delta I = |I_c^+| - |I_c^-|$  as a function of the fractional-order  $\alpha$  in a STT memristor. For an ideal memristor ( $\alpha = 1$ ), there is no asymmetry ( $\Delta I = 0$ ).

Applying the sinusoidal current source  $i(t) = A \cos(\omega t)$  with  $A = 2Q_0\omega^\alpha$  across the memristor, the corresponding memristor charge is given by Eq. (11). Then, we have

$$q(t) = D_t^{-\alpha} i(t) = D_t^{-\alpha} A \cos(\omega t) = 2Q_0 \cos\left(\omega t - \frac{\alpha}{2}\pi\right). \quad (12)$$

When  $\alpha = 1$ ,  $q(t) = 2Q_0 \cos(\omega t - \frac{1}{2}\pi) = 2Q_0 \sin(\omega t)$ , so the initial charge  $q(t=0) = 0$ . As can be clearly seen in Fig. 3, the sweeping range ( $4Q_0$ ) of  $q(t)$  is four times as great as the separation ( $Q_0$ ) between the breakpoint and the origin. Such a full range sweep ensures a thorough switching from one memristance to another in the STT memristor junction, which is extremely vital in applications such as MRAMs.

In Fig. 3, the memristor  $\varphi$ - $q$  curve traverses from  $q = 0$  at  $t = 0$  to  $q = 2Q_0$  at  $t = \pi/\omega$ . Starting from  $q(0) = 0$  at  $t = 0$ , the memristor charge  $q(t)$  increases along the lower branch while maintaining a constant high memristance value of  $R_{AP}$  until it reaches the breakpoint at  $q = Q_0$  where it switches abruptly to the upper branch and continues to increase, with the constant low memristance value of  $R_P$ , until it reaches the maximum value of  $q(t) = 2Q_0$  at  $t = \pi/(2\omega)$  corresponding to the end of the first 1/4 cycle (corresponding to the Time Label 0→1→2→3) of the sinusoidal charge  $q(t)$ . In Fig. 3(d), the corresponding chord memristance<sup>12,13</sup> remains constant at  $R_{AP}$  before the voltage switching take place at  $I_c^+$  and at  $R_P$  after  $I_c^+$ . The chord memristance is defined as the slope of a straight line connecting the corresponding point to the origin in the  $v$ - $i$  plane.<sup>12,13</sup> Observe also that the switching occurs instantaneously in this case in view of the discontinuity in the slope of the  $\varphi$ - $q$  curve at the breakpoint  $q(t=t_1) = Q_0$  at  $t = t_1$ . In the 2nd 1/4 cycle (Label 3→4→5), the  $\varphi$ - $q$  curve traverses back from  $q(t) = 2Q_0$  at  $t = \pi/(2\omega)$  to  $q(t) = 0$  at  $t = \pi/\omega$ , and both the current  $i(t)$  and voltage  $v(t)$  change their signs. When the  $\varphi$ - $q$  curve goes through the breakpoint at  $Q_0$  again, the corresponding voltage  $v(t)$  switches abruptly from the upper branch ( $R_P$ ) to the lower one ( $R_{AP}$ ) at  $I_c^-$ . Obviously, the two switching points in the  $v$ - $i$  plane are symmetric ( $|I_c^+| = |I_c^-|$ ) because they correspond to the same breakpoint  $Q_0$  (but along the two different directions) in the  $\varphi$ - $q$  plane. In the remaining half cycle (Label 5→6→7→8→9), the  $v$ - $i$  curve is a straight line without any switching as the slope of the  $\varphi$ - $q$  curve maintains a constant high memristance value of  $R_{AP}$  until it reaches the origin.

Figure 3(d) shows typically a pinched hysteresis loop, i.e., double-valued Lissajous figure of  $[v(t), i(t)]$  for all times  $t$  except when it passes through the origin, where the loop is pinched.<sup>13</sup> Obviously, the STT junction bears the fingerprint of a memristor and should be modelled as a memristor.

As described above, we transcribe the corresponding loci of the memristance  $R(t)$  from the pinched hysteresis loop into the  $R$ - $i$  plane. What we obtain is a rectangular resistance hysteresis loop shown in Fig. 3(b). Such a rectangular loop is symmetric ( $|I_c^+| = |I_c^-|$ , when  $\alpha = 1$ ), which is quite different from the measured one ( $|I_c^+| \neq |I_c^-|$ ) in the STT junction as shown in Fig. 2. Such a difference encourages us to guess a real-world STT junction which may not be described as an ideal memristor. Next, we will investigate the STT memristor's fractional-order model when  $0 < \alpha < 1$ .

Especially when the fractional-order  $\alpha = 0.8$ ,  $q(t) = 2Q_0 \cos(\omega t - \frac{\alpha}{2}\pi) = 2Q_0 \cos(\omega t - \frac{0.8}{2}\pi)$ , which is drawn in Fig. 4(e). Obviously,  $q(t)$  is shifted by  $0.4\pi$  along the  $t$  axis. Such a shift causes an asymmetric shifts ( $|I_c^+| \neq |I_c^-|$ ) of the two switching points of the  $v$ - $i$  and  $R$ - $i$  curves although the breakpoint  $Q_0$  of the  $\varphi$ - $q$  is fixed.

Concretely,  $q(t_1) = Q_0$ , that is

$$2Q_0 \cos\left(\omega t_1 - \frac{\alpha}{2}\pi\right) = Q_0, \quad (13)$$

$$\Delta I = |I_c^+| - |I_c^-| = 2Q_0 \omega^{0.8} \cos\left(\frac{3.4\pi}{6}\right). \quad (14)$$

Generally, for any  $0 < \alpha < 1$ ,

$$I_c^+ = i(t_1) = 2Q_0 \omega^\alpha \cos(\omega t_1) = 2Q_0 \omega^\alpha \cos\left(\frac{1+3\alpha}{6}\pi\right), \quad (15)$$

$$I_c^- = i(t_3) = 2Q_0 \omega^\alpha \cos(\omega t_3) = 2Q_0 \omega^\alpha \cos\left(\frac{5+3\alpha}{6}\pi\right), \quad (16)$$

$$\begin{aligned} \Delta I &= |I_c^+| - |I_c^-| \\ &= 2Q_0 \omega^\alpha \left[ \cos\left(\frac{1+3\alpha}{6}\pi\right) - \cos\left(\frac{5+3\alpha}{6}\pi\right) \right]. \end{aligned} \quad (17)$$

In Fig. 5, the asymmetry  $\Delta I = |I_c^+| - |I_c^-|$  is shown as a function of the fractional-order  $\alpha$ . The asymmetry needs to be normalized for a fair comparison due to the assumption  $A = 2Q_0\omega^\alpha$  (the amplitude  $A$  is a function of the frequency  $\omega$ ). For an ideal memristor ( $\alpha = 1$ ), there is no asymmetry ( $\Delta I = 0$ ). With the increase in  $\omega$ , the asymmetry reaches its maximum at different fractional-orders.

The similarity between such an asymmetric rectangular  $R$ - $i$  curve in this figure and the measured one in Fig. 2 reveals that a STT junction is not an ideal memristor, in which  $\alpha = 1$ .

The STT junctions have been widely made<sup>8-11</sup> since Slonczewski and Berger originated the STT theory in 1996.<sup>6,7</sup> So far, nobody called the STT junction a fractional memristor. It is our original contribution to first concept the fractional memristor based on the differential conformal transformation in the fractional order and proved that a typical STT junction is a 0.8 fractional memristor.

In conclusion, compared to the (traditional integer-order or ideal) memristor, the fractional memristor has the following advantages: (1) The fractional memristor is a real electrical element that is not ideal; (2) Deep physical understanding would be possible to develop a reliable commercial product for real-world applications [for example, the switching asymmetry in the STT MRAM (Magnetic Random Access Memory) could be modelled accurately by the fractional memristor and then reduced accordingly based on its physical origin]; (3) The fractional memristor representing the intermediate cases can seamlessly fill the gaps between the integer-order elements in the so-called Triangular Periodic Table of Elementary Circuit Elements, which is important to categorize the existing circuit elements and predict new elements.<sup>12</sup>

This research was partially conducted in an EC Grant “Re-discover a periodic table of elementary circuit elements,” PIFI-GA-2012-332059; Scientist-in-Charge: Professor F. Z. Wang and Marie Curie Fellow: Professor L. Chua. We wish to thank Professor Ivo Petras, Technical University of Kosice, for a useful conversation at Cambridge in March 2016.

- <sup>1</sup>L. Chua, “Memristor—the missing circuit element,” *IEEE Trans. Circuit Theory* **18**(5), 507–519 (1971).
- <sup>2</sup>K. B. Oldham and J. Spanier, *The Fractional Calculus* (Academic Press, New York, 1974).
- <sup>3</sup>I. Podlubny, *Fractional Differential Equations* (Academic Press, San Diego, 1999).
- <sup>4</sup>I. Petras, I. Podlubny, P. O’Leary, L. Dorcak, and B. Vinagre, *Analogue Realization of Fractional Order Controllers* (FBERG Technical University of Kosice, 2002).
- <sup>5</sup>M. Abdelouahab, R. Lozi, and L. Chua, “Memfractance: A mathematical paradigm for circuit elements with memory,” *Int. J. Bifurcation Chaos* **24**, 1430023 (2014).
- <sup>6</sup>J. C. Slonczewski, “Current-driven excitation of magnetic multilayers,” *J. Magnetism Magnetic Mater.* **159**(1–2), L1 (1996).

- <sup>7</sup>L. Berger, “Emission of spin waves by a magnetic multilayer traversed by a current,” *Phys. Rev. B* **54**, 9353 (1996).
- <sup>8</sup>G. D. Fuchs, N. C. Emley, I. N. Krivorotov, P. M. Braganca, E. M. Ryan, S. I. Kiselev, J. C. Sankey, D. C. Ralph, R. A. Buhrman, and J. A. Katine, “Spin-Transfer Effects in Nanoscale Magnetic Tunnel Junctions,” *Appl. Phys. Lett.* **85**, 1205–1207 (2004).
- <sup>9</sup>Y. Huai, D. Apalkov, Z. Diao, Y. Ding, and A. Panchula, “Structure, materials and shape optimization of magnetic tunnel junction devices: Spin-transfer switching current reduction for future magnetoresistive random access memory,” *Jpn. J. Appl. Phys.* **45**(5A), 3835–3841 (2006).
- <sup>10</sup>X. Li, Z. Zhang, Q. Y. Jin, and Y. Liu, “Spin-torque-induced switching in a perpendicular GMR nanopillar with a soft core inside the free layer,” *New J. Phys.* **11**, 023027 (2009).
- <sup>11</sup>H. Meng and J. Wang, “Asymmetric spin torque transfer in nano GMR Device with perpendicular anisotropy,” *IEEE Trans. Magn.* **43**(6), 2833 (2007).
- <sup>12</sup>F. Z. Wang, “A triangular periodic table of elementary circuit elements,” *IEEE Trans. Circuits Syst.* **60**(3), 616–623 (2013).
- <sup>13</sup>L. Chua, “Resistance switching memories are memristors,” *Appl. Phys. A* **102**(4), 765–783 (2011).
- <sup>14</sup>L. Chua, “If it’s pinched it’s a memristor,” *Semicond. Sci. Technol.* **29**(10), 104001 (2014).